A multidimensional pseudospectral method for optimal control of quantum ensembles

Justin Ruths and Jr-Shin Li[a)]
Department of Electrical and Systems Engineering, Washington University in St. Louis, St. Louis, Missouri, 63130 USA

(Received 8 August 2010; accepted 22 December 2010; published online 28 January 2011)

In our previous work, we have shown that the pseudospectral method is an effective and flexible computation scheme for deriving pulses for optimal control of quantum systems. In practice, however, quantum systems often exhibit variation in the parameters that characterize the system dynamics. This leads us to consider the control of an ensemble (or continuum) of quantum systems indexed by the system parameters that show variation. We cast the design of pulses as an optimal ensemble control problem and demonstrate a multidimensional pseudospectral method with several challenging examples of both closed and open quantum systems from nuclear magnetic resonance spectroscopy in liquid. We give particular attention to the ability to derive experimentally viable pulses of minimum energy or duration. © *2011 American Institute of Physics*. [doi:10.1063/1.3541253]

I. INTRODUCTION

The complexity inherent in pulse design for manipulating quantum systems limits the analytic tractability of solutions and motivates the study of computational methods to address such problems. The necessity of numerical methods is even more clear when parameter variations are incorporated into modeling the system dynamics. These variations are prevalent in quantum systems in many forms and vital to consider in order for theoretical prediction to match experimental outcome. For example, systems in nuclear magnetic resonance (NMR) spectroscopy and magnetic resonance imaging (MRI) exhibit frequency (Larmor) dispersion, radio frequency (rf) field inhomogeneity, as well as relaxation rate and spin coupling variation. The inclusion of these perturbations requires us to consider a pulse design problem for an ensemble of quantum systems indexed by the physical parameters showing variation.[1]

A variety of methods have been developed in the past decades of research in pulse sequence design. Theoretical methods, such as composite pulses and hyperbolic secant pulses,[2–6] and custom numerical schemes[7,8] have been used within the pulse design community. The well-known Shinnar–Le Roux (SLR) algorithm in MRI designs frequency selective pulses via polynomial approximation based on small tip-angle approximations and spinor representation.[9] Such specific methods, however, are not directly extendible to include other variations. For example, designing extensions to the SLR algorithm using Fourier synthesis techniques to also compensate for rf inhomogeneity is both challenging and involved.[10] More recently pulse design has been approached from a perspective of optimal control[11–17] and gradient-type methods have been successfully applied to systems with parameter variations.[18] Although the optimal control formulation is arbitrarily general, extensions of gradient methods require investment to recompute and reimplement evolution propagators and objective gradients.

As experiments become more demanding in terms of pulse design, compensating for additional variations will be of particular interest and of increasing importance. The limitations of current pulse design methods motivate the need for a more flexible numerical optimization method, which can be adopted quickly and used effectively. In our previous work, we developed a pseudospectral method for solving idealized pulse design problems of quantum systems that is straightforward to implement, relatively robust to local minima, and exhibits fast convergence rates.[19] Here, we describe a multidimensional extension of the pseudospectral method to consider more realistic pulse design problems for quantum systems exhibiting parameter variation.

In Sec. II, we provide a general mathematical model for pulse design and review the pseudospectral method as well as introduce the ensemble extension. Section III illustrates several of the key advantages and features of this newly developed method using canonical examples from NMR spectroscopy in liquids.

II. ENSEMBLE PSEUDOSPECTRAL METHOD FOR PULSE DESIGN

We consider quantum dynamics under the Markovian approximation. In this case, the system state can be represented by a vector $x \in \mathbb{R}^n$, which evolves according to

$$\dot{x} = \left[\mathcal{H}_d + \sum_{i=1}^{m} u_i(t)\mathcal{H}_i\right]x, \tag{1}$$

where $u_i(t)$, $i = 1, \ldots, m$ are electromagnetic pulses and $\mathcal{H}_d, \mathcal{H}_i \in \mathbb{R}^{n\times n}$ are square matrices representing the system Hamiltonian.[19]

In practice the system Hamiltonian and, therefore, the matrices $\mathcal{H}_d$ and $\mathcal{H}_i$ are not uniform across the systems of

a)Electronic address: jsli@seas.wustl.edu.

interest. Rather these quantities show variations in system parameters, such as frequency, rf scaling, relaxation rates, and spin coupling constants, due to different spatial locations and chemical environments. Consolidating these individual factors into a parameter vector $s \in \Omega \subset \mathbb{R}^d$, the corresponding pulse design problem with parameter variation can be written as a new class of optimal ensemble control problem,

$$\begin{aligned} \min \quad & \int_\Omega \left[\varphi(T, x(T,s)) + \int_0^T \mathcal{L}(x(t,s), u(t))\, dt\right] ds, \\ \text{s.t.} \quad & \frac{d}{dt}x(t,s) = \left[\mathcal{H}_d(s) + \sum_{i=1}^m u_i(t)\mathcal{H}_i(s)\right] x(t,s), \\ & e(x(0,s), x(T,s)) = 0, \\ & g(x(t,s), u(t)) \le 0, \quad \forall\, s \in \Omega,\ t \in [0,T], \end{aligned} \tag{2}$$

where φ and $\mathcal{L}$ are the real-valued functions denoting the terminal (at the final time, T) and running cost terms of the general objective function, respectively, e represents endpoint constraints, and g denotes path constraints. The general problem formulation in Eq. (2) is sufficient to describe an arbitrary practical pulse design problem with any number of constraints.

Solving this optimal control problem in the continuous-time and parameter domain analytically is generally intractable and we, therefore, look for computational methods to derive numerical solutions. The remainder of this section will present how the multidimensional pseudospectral method effectively discretizes the optimal control problem in Eq. (2) in both the time and parameter spaces. We first review the fundamental pseudospectral method without consideration for parameter variation (see Ref. 19) and then subsequently extend these techniques to include optimal sampling in the ensemble case.

A. Pseudospectral method

The overarching goal of the pseudospectral method is to convert the continuous-time optimal control problem in Eq. (2) into a constrained algebraic optimization problem, which can be solved efficiently by existing nonlinear numerical optimization solvers. The pseudospectral method was originally developed to solve problems in fluid dynamics, and since then the related concepts have been successfully applied to many areas of science and engineering.[20–23] Pseudospectral discretization methods use orthogonal polynomial expansions to approximate the states and controls of the system and thereby inherit the spectral accuracy characteristic of such expansions (the kth coefficient of the expansion decreases faster than any inverse power of k).[24] Using recursive properties unique to certain classes of orthogonal polynomials, e.g., Legendre and Chebyshev, derivatives of the states can again be expressed in terms of the orthogonal polynomial expansions, making it possible to accurately approximate the differential equation that describes the dynamics with an algebraic relation imposed at a small number of discretization points. An appropriate choice of these discretization points, or nodes, facilitates the approximation of the states as well as ensures accurate numerical integration.

We first transform the original problem from the time domain $t \in [0, T]$ to the rescaled domain $t \in [-1, 1]$ on which the orthogonal polynomials are defined. We then approximate the states and controls by truncated Nth-order expansions in terms of Legendre orthogonal polynomials,

$$x(t) \approx P_N x(t) = \sum_{k=0}^N \tilde{x}_k L_k(t), \tag{3}$$

$$u(t) \approx P_N u(t) = \sum_{k=0}^N \tilde{u}_k L_k(t), \tag{4}$$

where $L_k(t)$ is the kth Legendre polynomial. Our choice to use the Legendre polynomials dictates, we compute the integral term of the cost function using Legendre–Gauss–Lobatto (LGL) quadrature, in which the integral is approximated by a summation of the integrand evaluated at a specific set of $N + 1$ nodes,

$$\int_{-1}^1 f(t)\, dt \approx \sum_{i=0}^N f(t_i) w_i, \qquad w_i = \int_{-1}^1 \ell_i(t)\, dt, \tag{5}$$

where f is a continuous function on $[-1, 1]$, w_i are discrete weights, and $\ell_i(t)$ is the ith Lagrange polynomial, discussed below.[25] The set of LGL nodes, $\Gamma^{\mathrm{LGL}} = \{t_i : \dot{L}_N(t)|_{t_i} = 0, i = 1, \ldots, N-1\} \bigcup \{-1, 1\}$, is determined by the derivative of the Nth-order Legendre polynomial, $\dot{L}_N(t)$, and the endpoints, -1 and 1.[24] This choice of nodes makes the integral approximation exact for $f \in \mathbb{P}_{2N-1}$, the set of polynomials of degree $2N - 1$ or less.

Although the Legendre expansions (3) and (4) provide an accurate approximation of the states and controls, they do not provide a straightforward way of evaluating these functions at specific points, such as at the LGL nodes, which is required in the quadrature approximation (5) of the integral terms of the cost function. To overcome this, we approximate these Legendre expansions with interpolating polynomials, which, by definition, are equal to the Legendre expansions at the interpolation nodes. Because any interpolating polynomial can be represented by Lagrange polynomials, we can approximate the state and control as

$$P_N x(t) \approx I_N x(t) = \sum_{k=0}^N \bar{x}_k \ell_k(t), \tag{6}$$

$$P_N u(t) \approx I_N u(t) = \sum_{k=0}^N \bar{u}_k \ell_k(t), \tag{7}$$

where the coefficients $\bar{x}_k$ and $\bar{u}_k$ are defined by $P_N x(t_k) = I_N x(t_k) = \bar{x}_k$ and $P_N u(t_k) = I_N u(t_k) = \bar{u}_k$, respectively, because $\ell_k(t_i) = \delta_{ki}$, where δ_{ki} is the Kronecker delta function.[26] Using this second approximation, we can compute the integrand of the cost function integral at the LGL nodes and $\bar{x}_k$ and $\bar{u}_k$ become the decision variables of the subsequent discretized optimization problem.

The Lagrange polynomials with the choice of LGL interpolating nodes can be expressed in terms of the

Legendre polynomials, which is critical so that the pseudospectral method inherits the special derivative and spectral accuracy properties of the orthogonal polynomials despite using Lagrange interpolating polynomials. Given $t_k \in \Gamma^{\mathrm{LGL}}$, we can express the Lagrange polynomial as[27]

$$\ell_k(t) = \frac{1}{N(N+1)L_N(t_k)} \frac{(t^2-1)\dot{L}_N(t)}{t-t_k}. \tag{8}$$

The derivative of $I_N x(t)$ in Eq. (6) at $t_j \in \Gamma^{\mathrm{LGL}}$ is then

$$\frac{d}{dt} I_N x(t_j) = \sum_{k=0}^{N} \bar{x}_k \dot{\ell}_k(t_j) = \sum_{k=0}^{N} D_{jk} \bar{x}_k, \tag{9}$$

where D is the constant $(N+1)\times(N+1)$ differentiation matrix.[28]

B. Multidimensional extension & ensemble sampling

The optimal ensemble control problem in Eq. (2) includes another dimension of continuity from the parameter domain, $s \in \Omega \subset \mathbb{R}^{\mathrm{d}}$, which must be discretized (or sampled) to be solved numerically. First consider the case of a single parameter variation, $x(t,s) \in \mathbb{R}^n$, $s \in [a,b] \subset \mathbb{R}$. The ensemble extension of Eq. (6) using a two-dimensional interpolation approximation is

$$\begin{aligned} x(t,s) \approx I_{N\times N_s} x(t,s) &= \sum_{k=0}^{N} \bar{x}_k(s)\ell_k(t) \\ &\approx \sum_{k=0}^{N} \left(\sum_{r=0}^{N_s} \bar{x}_{kr}\ell_r(s) \right) \ell_k(t). \end{aligned} \tag{10}$$

The approximate derivative from Eq. (9) at the LGL nodes in the respective t and s domains, $t_i \in \Gamma^{\mathrm{LGL}}$ and $s_j \in \Gamma^{\mathrm{LGL}}_{N_s}$, is

$$\begin{aligned} \frac{d}{dt} I_{N\times N_s} x(t_i,s_j) &= \sum_{k=0}^{N} D_{ik} \left(\sum_{r=0}^{N_s} \bar{x}_{kr}\ell_r(s_j) \right) \\ &= \sum_{k=0}^{N} D_{ik}\bar{x}_{kj}, \end{aligned} \tag{11}$$

where $\bar{x}_{kj} = x(t_k, s_j)$. In Eqs. (10) and (11), we have effectively used a two-dimensional interpolating grid at the $N+1$ and N_s+1 LGL nodes in time and the parameter, respectively. Using Eqs. (10) and (11) in conjunction with the LGL quadrature rule in Eq. (5), we summarize the pseudospectral discretization of the optimal ensemble control problem as

$$\begin{aligned} \min \quad & \frac{b-a}{2} \sum_{r=0}^{N_s} \left[\varphi(T, \bar{x}_{Nr}) + \frac{T}{2} \sum_{i=0}^{N} \mathcal{L}(\bar{x}_{ir}, \bar{u}_i) w_i^N \right] w_r^{N_s} \\ \text{s.t.} \quad & \sum_{k=0}^{N} D_{jk}\bar{x}_{kr} = \frac{T}{2} \left[\mathcal{H}_d^r + \sum_{i=1}^{m} \bar{u}_{ij} \mathcal{H}_i^r \right] \bar{x}_{jr}, \\ & e(\bar{x}_{0r}, \bar{x}_{Nr}) = 0, \\ & g(\bar{x}_{jr}, \bar{u}_j) \le 0, \quad \begin{matrix} \forall\ j \in \{0,1,\ldots,N\} \\ r \in \{0,1,\ldots,N_s\} \end{matrix}, \end{aligned} \tag{12}$$

where $\mathcal{H}_d^r$ and $\mathcal{H}_i^r$ are $n \times n$ matrices representing the Hamiltonians with respect to the rth parameterized system and $\bar{u}_{ij}$ is the value of the control function u_i at the jth LGL node t_j.

It is straightforward to extend this interpolating structure to accommodate parameter spaces of higher dimension, $\mathbf{s} = (s_1, s_2, \ldots, s_d)' \in \Omega \subset \mathbb{R}^{\mathrm{d}}$, $d > 1$. In this general case

$$\begin{aligned} x(t,\mathbf{s}) \approx I_{N\times N_{s_1}\times\cdots\times N_{s_d}} x(t,\mathbf{s}) &= \sum_{k=0}^{N} \bar{x}_k(\mathbf{s})\ell_k(t) \\ &= \sum_{k=0}^{N} \sum_{r_1=0}^{N_{s_1}} \cdots \sum_{r_d=0}^{N_{s_d}} \bar{x}_{kr_1\ldots r_d} \ell_{r_d}(s_d)\cdots\ell_{r_1}(s_1)\ell_k(t). \end{aligned}$$

III. EXAMPLES IN NMR

We now illustrate several of the key properties of the pseudospectral method for optimal control of quantum ensembles through representative examples from NMR in liquids. These systems exhibiting parameter variation form challenging problems in quantum control. The ability to solve them with the method presented here demonstrates it as a universal method for optimal pulse design. Specifically, we design rf pulses for systems modeled by the Bloch equations with Larmor dispersion in the presence of rf inhomogeneity, which has direct applications to NMR, MRI, quantum information processing, and quantum optics. We also design pulses that achieve optimal coherence transfer between a pair of heteronuclear spins with variation in relaxation rates and spin coupling strengths. We first present the corresponding ensemble systems and then highlight the advantages of the pseudospectral method with simulation results.

A. Broadband pulse design in the presence of rf inhomogeneity

The evolution of the bulk magnetization of a sample of nuclear spins follows the Bloch equations.[29] As pulse design requirements are becoming increasingly more demanding, it is necessary to consider effects, such as Larmor dispersion and rf inhomogeneity, to ensure that theoretical prediction matches experimental outcomes. Differences in the chemical environment within the sample can cause variations in the natural frequency and is observed at the macroscopic level as Larmor dispersion. Equipment imperfection can cause signal attenuation and results in amplitude scaling of the rf pulse across the sample, called rf inhomogeneity. We formulate robust pulse design compensating for Larmor dispersion and rf inhomogeneity as the following optimal ensemble control problem,

$$\begin{aligned} \max \quad & \mathcal{J} \\ \text{s.t.} \quad & \frac{d}{dt} \begin{bmatrix} x(t,\omega,\epsilon) \\ y(t,\omega,\epsilon) \\ z(t,\omega,\epsilon) \end{bmatrix} = \begin{bmatrix} 0 & -\omega & \epsilon u \\ \omega & 0 & -\epsilon v \\ -\epsilon u & \epsilon v & 0 \end{bmatrix} \begin{bmatrix} x(t,\omega,\epsilon) \\ y(t,\omega,\epsilon) \\ z(t,\omega,\epsilon) \end{bmatrix}, \\ & [x(0,\omega,\epsilon)\ y(0,\omega,\epsilon)\ z(0,\omega,\epsilon)]' = [0\ 0\ 1]', \\ & \sqrt{u^2(t)+v^2(t)} \le A,\ \forall\, t \in [0,T], \end{aligned} \tag{13}$$

where $\mathcal{J}$ is the chosen cost function, $[x\ y\ z]$ is the state vector representing the magnetization vector over time $t \in [0, T]$ and parameterized by ω and ϵ, T is the terminal time (or pulse duration), which can either be fixed or free to vary within an interval $[0, T_{\max}]$, $\omega \in [-B, B]$, $B > 0$ is the offset frequency in the rotating frame with respect to the central frequency, $\epsilon \in [1-\delta, 1+\delta]$, $\delta \in [0, 1]$ is the scaling factor for the rf pulse; u and v are the components of the rf pulse applied in the y and x axis, respectively, and A is the maximum allowable amplitude.

A fundamental pulse in NMR experiments is a $\pi/2$ pulse, which corresponds to a control law $[u(t), v(t)]$ that rotates the bulk magnetization vector initially from the equilibrium state $[0\ 0\ 1]'$ onto the transverse plane, e.g., $[1\ 0\ 0]'$. Therefore, we seek to design the single rf pulse $[u(t), v(t)]$ that takes the continuum of spins with frequencies distributed in $\omega \in [-B, B]$ and in the presence of different rf scalings, $\epsilon \in [1-\delta, 1+\delta]$, from the z-axis to the x-axis. Such a pulse is called a broadband excitation pulse robust to rf inhomogeneity. To this end, we select an appropriate objective to maximize the average value of the x-component of the spin population magnetization at the terminal time,

$$\mathcal{J}_{avg} = \frac{1}{4\delta B}\int_{1-\delta}^{1+\delta}\int_{-B}^{B} x(T, \omega, \epsilon)\, d\omega\, d\epsilon. \tag{14}$$

B. Robust coherence transfer

The coherence transfer between two spins is a fundamental step to multidimensional NMR spectroscopy. In protein NMR spectroscopy, large transverse relaxation rates can cause degraded sensitivity and thereby limits the size of macromolecules available for study.[15] We highlight several important properties of the pseudospectral method through pulse design of coupled heteronuclear spin systems with and without cross-correlated relaxation effects. The single-valued parameter systems of the following relaxation-optimized pulse design problems have been studied analytically and the corresponding optimal controls are denoted ROPE in Ref. 30 and CROP in Ref. 31, respectively. Although these analytic controls are only valid for the single-valued parameter systems, i.e., without variation, we use them as a benchmark to indicate the upper bound on the expected coherence transfer of the ensemble quantum systems. The following systems are described in detail in Ref. 19, and we extend them now to consider the more realistic case in which parameter variations in relaxation rates and coupling constants are present.

1. Coherence transfer without cross-correlated relaxation

We focus on large molecules in the so-called spin diffusion limit, where longitudinal relaxation rates are negligible compared to transverse. The most important transverse relaxation mechanisms are dipole–dipole (DD) and chemical shift anisotropy (CSA) relaxation. We initially ignore the cross-correlation rates caused by interference between DD and CSA relaxation. The optimal ensemble control problem corresponding to designing a relaxation-optimized pulse $[u_1(t), u_2(t)]$ to maximize the coherence transfer in the presence of variation in relaxation rates and spin coupling can be formulated as

$$\begin{aligned}
\max\ & \mathcal{J}_{avg} = \frac{1}{2\delta(\xi_2-\xi_1)}\int_{1-\delta}^{1+\delta}\int_{\xi_1}^{\xi_2} x_4(T, \xi, J)\, d\xi\, dJ \\
\text{s.t.}\ & \begin{bmatrix}\dot{x}_1\\ \dot{x}_2\\ \dot{x}_3\\ \dot{x}_4\end{bmatrix} = \begin{bmatrix}0 & -u_1 & 0 & 0\\ u_1 & -\xi & -J & 0\\ 0 & J & -\xi & -u_2\\ 0 & 0 & u_2 & 0\end{bmatrix}\begin{bmatrix}x_1\\ x_2\\ x_3\\ x_4\end{bmatrix}, \\
& x(0) = [1\ 0\ 0\ 0]', \\
& \sqrt{u_1^2(t) + u_2^2(t)} \le A,\ \forall t \in [0, T],
\end{aligned} \tag{15}$$

where $\mathcal{J}_{avg}$ is the objective that maximizes the average final value of x_4 across the ensemble; $x_i = x_i(t, \xi, J)$ are expectation values of the spin operators,[19] T is the final time, free to vary as a decision variable, $\xi \in [\xi_1, \xi_2]$ is the transverse autocorrelated relaxation rate, $J \in [1-\delta, 1+\delta]$, $\delta \in [0, 1]$, is the scalar coupling constant, u_1 and u_2 are the applied controls, and A is the maximum allowable amplitude.

2. Coherence transfer with cross-correlated relaxation

The more general case, in which cross-correlated relaxation is not neglected, leads to a modified formulation of the problem. Here we consider variation in the relaxation rate without variation in the spin coupling,

$$\begin{aligned}
\max\ & \mathcal{J}_{avg} = \frac{1}{(\xi_2-\xi_1)}\int_{\xi_1}^{\xi_2} x_6(T, \xi_a)\, d\xi_a \\
\text{s.t.}\ & \begin{bmatrix}\dot{x}_1\\ \dot{x}_2\\ \dot{x}_3\\ \dot{x}_4\\ \dot{x}_5\\ \dot{x}_6\end{bmatrix} = \begin{bmatrix}0 & -u_1 & u_2 & 0 & 0 & 0\\ u_1 & -\xi_a & 0 & -J & -\xi_c & 0\\ -u_2 & 0 & -\xi_a & -\xi_c & J & 0\\ 0 & J & -\xi_c & -\xi_a & 0 & -u_2\\ 0 & -\xi_c & -J & 0 & -\xi_a & u_1\\ 0 & 0 & 0 & u_2 & -u_1 & 0\end{bmatrix}\begin{bmatrix}x_1\\ x_2\\ x_3\\ x_4\\ x_5\\ x_6\end{bmatrix}, \\
& x(0) = [1\ 0\ 0\ 0\ 0\ 0]', \\
& \sqrt{u_1^2(t) + u_2^2(t)} \le A,\ \forall t \in [0, T],
\end{aligned} \tag{16}$$

where $\mathcal{J}_{avg}$ is the objective that maximizes the average final value of x_6 across the ensemble; $x_i = x_i(t, \xi_a)$ are expectation values of components of the spin operators, T is the final time, free to vary as a decision variable, $\xi_a \in [\xi_1, \xi_2]$ is the autocorrelated relaxation rate and ξ_c is the cross-correlation relaxation rate, J is the scalar coupling constant, u_1 and u_2 are the applied controls, and A is the maximum allowable amplitude.[19] To demonstrate, here we consider the case in which $\xi_c = 0.75\xi_a$ and $J = 1$.

C. Pseudospectral method features

In the following subsections, we show that the pseudospectral method finds effective solutions to the pulse

design problems listed above and, for problems in Eqs. (15) and (16), finds pulses that achieve robust coherence transfer near the analytic upper bound. Note that the features of the pseudospectral method described below are general to the method itself and not related to the specific system to which it is applied. We highlight these key attributes using the problems above and motivate why this is a universal method for deriving experimentally viable pulses for quantum systems.

1. Cost function flexibility

Within the scope of an optimal control problem, the selection of an appropriate cost function is particularly important. In addition, there are often different choices for the objective associated with the same goal. For example, in the Bloch system consider the cost functional that minimizes the error between a desired target, $x_d(\omega, \epsilon)$, and the terminal state value, i.e., min $\mathcal{J}_{\text{err}}$,

$$\mathcal{J}_{\text{err}} = \frac{1}{4\delta B} \int_{1-\delta}^{1+\delta} \int_{-B}^{B} |x_d(\omega, \epsilon) - x(T, \omega, \epsilon)| \, d\omega \, d\epsilon. \quad (17)$$

While minimizing Eq. (17) and maximizing Eq. (14) appear to imply the same optimization target when $x_d(\omega, \epsilon) = 1$, in practice the numerical properties of these two cost functions causes solvers to deal with these differently. Moreover, there are reasons to consider several optimization goals and, therefore, a number of cost function choices. For example, it can be of interest to develop minimum-energy or minimum-time pulses. A combination of these objective choices can provide a tradeoff between their respective advantages.

A broadband $\pi/2$ pulse [see problem (13)] derived by the multidimensional pseudospectral method with $\mathcal{J} = \mathcal{J}_{\text{avg}}$, $A = 20$ kHz, $B = 20$ kHz, $\delta = 0.1$, and $T = 100$ μs is shown in Fig. 1. In implementation, the physical units of the systems are normalized to dimensionless parameters. For the Bloch system, we normalize by the maximum allowable amplitude, A, i.e., $\tilde{A} = 1$, $\tilde{B} = B/A$, and $\tilde{T} = TA \times 2\pi$ (2π accounts for converting units between Hz and radians/s). This normalized broadband $\pi/2$ pulse compensates for the offset $[-1, 1]$ and 10% rf inhomogeneity with maximum allowable amplitude $A = 1$ and duration $T = 4\pi$. Normalizing in this way leads to a more general formulation as the pulse in Fig. 1 can be scaled to any chosen maximum allowable amplitude.

Figure 2 shows a solution of the normalized Bloch system with a wider bandwidth $[-1.5, 1.5]$ without rf inhomogeneity corresponding to $\mathcal{J} = \mathcal{J}_{\text{avg}} - 0.5\mathcal{J}_{\text{E}}$, where the second term serves to minimize the energy of the controls normalized by the maximum allowed energy

$$\mathcal{J}_{\text{E}} = \frac{1}{A^2 T} \int_0^T u^2(t) + v^2(t) \, dt. \quad (18)$$

2. Smoothing

Due to the use of polynomial approximation, the pseudospectral method naturally finds continuous and smooth solutions. Smooth pulses are of particular interest because such controls are experimentally practical to implement on a scanner without losses. In NMR experiments, although a desired pulse may be intended to have an instantaneous step change, the physical limitations of hardware cause latency that in turn

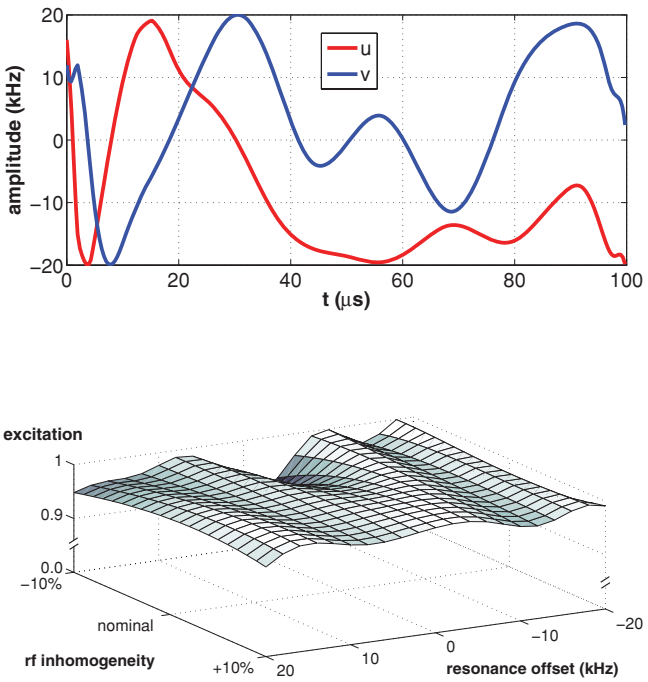

FIG. 1. The optimal ensemble pulse (a), shown as x and y rf components (conventionally $u = B_{1y}$ and $v = B_{1x}$), is robust to frequency variation on the interval $\omega \in [-20, 20]$ kHz and rf scaling on the interval $\epsilon \in [0.9, 1.1]$. The excitation profile (b), showing the terminal x-component of the magnetization spin vector, $x(T, \omega, \epsilon)$, has an average value of 0.98. This optimal ensemble pulse was developed by maximizing the excitation with $N = 24$, $N_\omega = 8$, and $N_\epsilon = 1$.

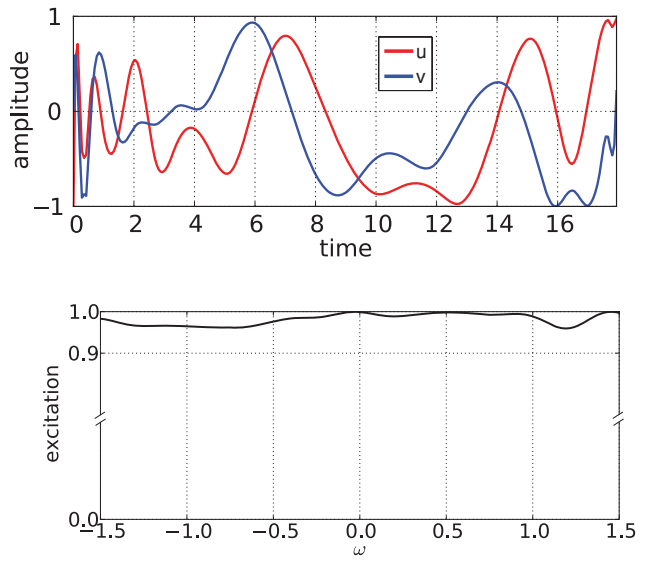

FIG. 2. The optimal ensemble pulse (a), shown as x and y rf components (conventionally $u = B_{1y}$ and $v = B_{1x}$), is robust to frequency variation on the interval $\omega \in [-1.5, 1.5]$. The excitation profile (b), showing the terminal x-component of the magnetization spin vector, $x(T, \omega, 1)$, has an average value of 0.98. This optimal ensemble pulse was developed by maximizing the excitation and minimizing energy with $N = 28$ and $N_\omega = 24$.

causes differences between experimental results and predicted outcomes. For example, the analytical ROPE solution to the coherence transfer problem in Eq. (15) features impulses at the beginning and end as well as sharp peaks in the middle, however, the pseudospectral method has been used to find smooth pulses that approximate the discontinuous ROPE solutions.[19,30]

Figure 3 illustrates smooth pseudospectral solutions to the normalized coherence transfer problem in Eq. (15) with $\xi \in [0, 2]$, fixed $J = 1$ (no variation in spin coupling), and amplitude bound $A = 20$. If we use the pseudospectral method with cost $\mathcal{J}_{\text{avg},}$ we obtain the fluctuating pulse shown in Fig. 3(a). If we use the same method with the hybrid cost $\mathcal{J} = \mathcal{J}_{\text{avg}} - \mathcal{J}_{\text{E},}$ we obtain the pulse shown in Fig. 3(b) with less oscillation. Both of these pulses achieve a similar ensemble performance and Fig. 3(c) depicts the coherence transfer corresponding to the hybrid objective pulse in Fig. 3(b). Including the minimum energy term in the objective yields a significantly more implementable and physically intuitive pulse. In most cases, there are a large (possibly uncountable) number of feasible solutions that achieve a similar performance, and it is experimentally advantageous to select from this large number the one that also minimizes energy.

Figure 4 shows a solution to the problem posed in Eq. (15) and corresponding coherence transfer for the two-dimensional ensemble problem with $\xi \in [0, 2]$ and $J \in [0.5, 1.5]$ using the same hybrid objective defined above. The transfer efficiency of the ensemble pulse derived with the pseudospectral method is robust to both parameter variations and still compares favorably with the upper bound achieved by the ROPE pulses.

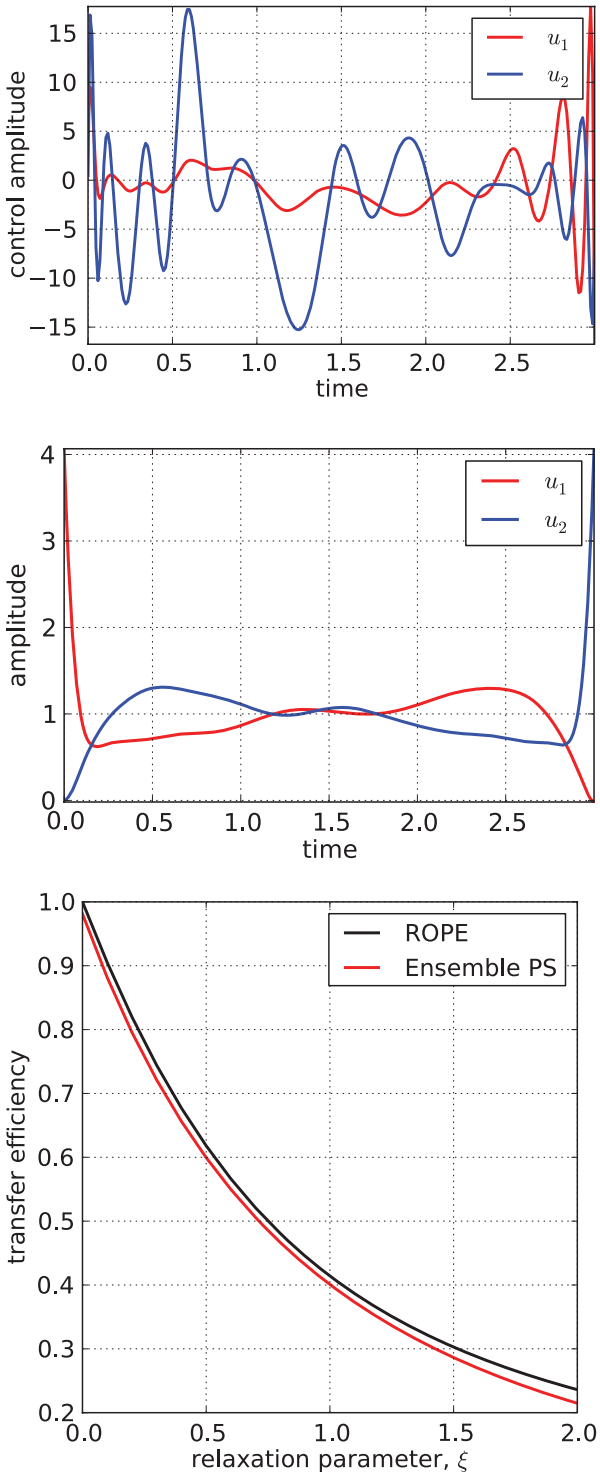

FIG. 3. The optimal ensemble pulses (a), (b) effectively compensate for all variations of ξ on the interval $[0, 2]$ with only minor losses in transfer efficiency (c) when compared to each analytic ROPE pulse (Ref. 30) efficiency for a single value of ξ ($N = 28$ and $N_\xi = 8$). The optimal ensemble pulse (a) was developed by maximizing the average transfer efficiency and the pulse (b) was developed by maximizing the average transfer efficiency and minimizing energy. The transfer efficiency (c) corresponds to the hybrid pulse in (b).

3. Numerical convergence

Applying pseudospectral methods to the original optimal control problem in Eq. (2) creates the discretized optimization given in Eq. (12). An important fundamental concern is to then show that the solutions of the discretized problem converge to solutions of the original optimal control problem as the number of discretization and sampling nodes increase. Convergence proofs for the pseudospectral method exist for only a few special classes of systems.[32] Since most quantum systems described by Eq. (2) do not fall within these classes, here we illustrate the convergence numerically. Figure 5 shows the convergence of the cost $\mathcal{J}_{\text{avg}}$, or performance, of the Bloch system in Eq. (13) as a function of the discretization in time (N) and parameter sampling (N_s), where for demonstration we have taken $N_s = N_\omega = N_\epsilon$. As expected at low sampling there is not a reliable ordering because the number of samples taken is not sufficient to characterize the parameter variation. However, for N and N_s large enough, Fig. 5 illustrates consistent convergence in both discretization and sampling.

4. Implementation and extension

The multidimensional pseudospectral method proposed for discretizing an optimal ensemble control problem is straightforward to implement and can be accomplished in virtually any computation environment. The optimizations shown here are solved in AMPL,[33] which is a specific syntax and program for expressing optimization problems,

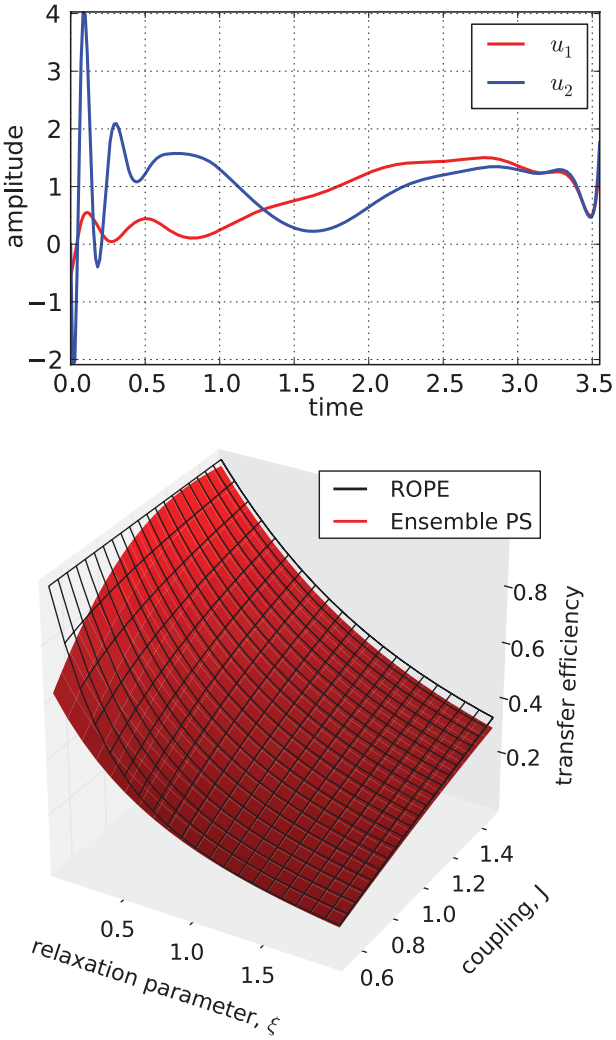

FIG. 4. The optimal ensemble pulse shown in (a) effectively compensates for all variations of ξ on the interval [0, 2] and J on the interval [0.5, 1.5] with comparable efficiency (b) to each ROPE pulse (Ref. 30) for a specific ξ and J. This optimal ensemble pulse was developed by maximizing average transfer efficiency and minimizing energy with $N = 24$, $N_\xi = 8$, and $N_J = 4$.

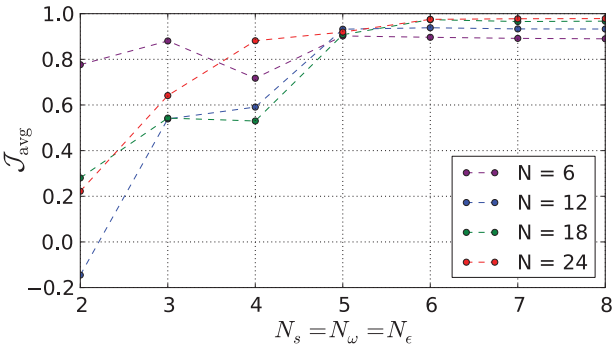

FIG. 5. The performance (J_{avg}) of the Bloch system, with $\omega \in [-1, 1]$ and $\epsilon \in [0.9, 1.1]$, converges as the discretization (N) and sampling (N_s) increase. For N and N_s large enough, the performance converges with increasing discretization and/or sampling. The initial scatter observed at low N_s is expected until a sufficient number of samples are taken to characterize the parameter variation (i.e., $N_s > 5$).

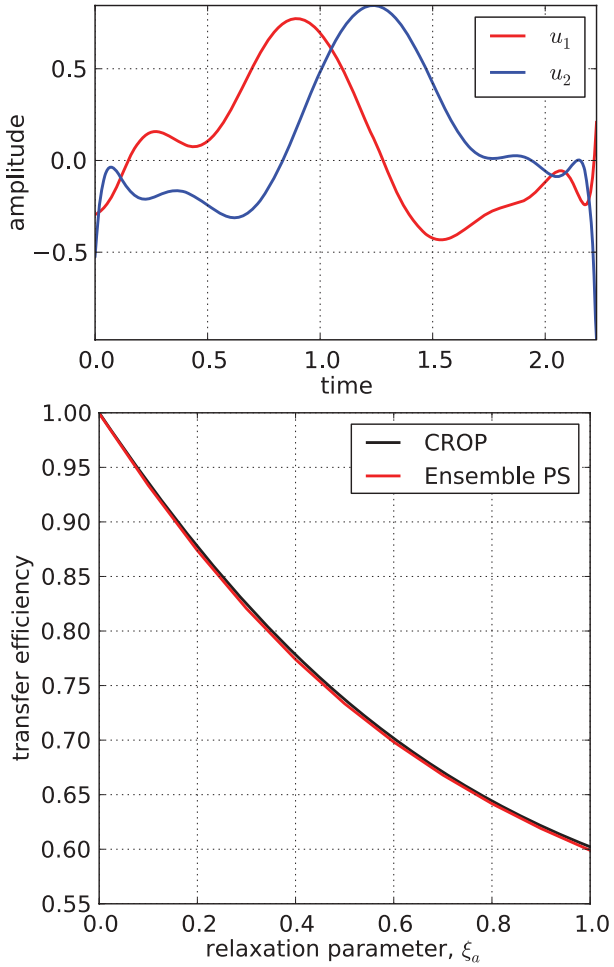

FIG. 6. The optimal ensemble pulse (a) effectively compensates for all variations of ξ_a ($\xi_c = 0.75\xi_a$) on the interval [0, 1] with only minor losses in the transfer efficiency (b) when compared to each analytic CROP pulse (Ref. 31) designed for a single value of ξ_a. This optimal ensemble pulse was developed with $N = 16$ and $N_{\xi_a} = 2$.

however, pseudospectral discretization can be implemented in a variety of languages including MATLAB, PYTHON, and C. Once familiar with the discretization and environment, the problem can be composed in very short amount of time. After a problem is fully implemented, modifying the code to be used with another system is straightforward. A major factor in the speed of implementation compared to existing methods, e.g., the gradient method,[12] is that the method does not require the explicit form of the gradient, for example, $(\partial\mathcal{J}/\partial u_1, \partial\mathcal{J}/\partial u_2)$ in the optimization problem in Eq. (15), which becomes difficult as hybrid cost functions are introduced. The small investment necessary to implement the pseudospectral method makes it readily accessible to experimental and theoretical researchers alike. Transforming the optimal ensemble control problem in Eq. (2) into a constrained nonlinear programing optimization in Eq. (12) enables researches to take advantage of mature and robust numerical solvers designed for such problems. Numerous such nonlinear programing solvers exist such as KNITRO, which is used here.

5. Computational complexity

All of the pseudospectral optimizations in this paper exhibit relatively coarse discretization in the time domain (N) and sampling in the parameter domain (N_s). Figure 6 illustrates a solution to the normalized ensemble coherence transfer problem with cross-correlated relaxation as in Eq. (16) with $\xi_a \in [0, 1]$, $\xi_c = 0.75\xi_a$, and $J = 1$. The optimal coherence transfer of the pseudospectral pulse matches favorably with that the single-ξ_a optimal CROP pulse.[31] The optimization corresponding to Fig. 6 achieves a level of spin transfer with an average of 3×10^{-3} deviation from the optimal upper bound with only $N = 16$ and $N_{\xi_a} = 2$. Maintaining low sampling numbers is of particular interest as the computational complexity of an ensemble problem of high dimension grows quickly. The optimization in Fig. 6 has (17 nodes in t) $\times$ (3 nodes in ξ) $\times$ (2 controls + 6 states) = 408 independent decision variables, which is well within the size of optimization typically handled by nonlinear solvers.

IV. CONCLUSION

As pulse sequence design for control of quantum nsembles becomes more complex, such as the consideration of parameter variation, these challenging problems require increasingly more flexible numerical methods to find solutions. We present here a highly adaptable framework based on pseudospectral discretization methods, which converts the continuous-time optimal control problem into a constrained algebraic optimization problem. This methodology admits a natural extension to consider optimal sampling for ensembles of quantum systems indexed by variations in parameter values. In our previous work, we illustrated the ability of the pseudospectral method to match the performance of analytic and gradient-based control pulses while at the same time allowing for more diverse cost function options and faster convergence rates.[19] Here, we developed a multidimensional extension of pseudospectral methods to the ensemble case, where the quantum systems are characterized by variations in natural frequency, rf scaling, relaxation rates, and coupling constants. The systems and solutions illustrated here are more than examples to motivate the pseudospectral method. They are relevant and practical pulse design solutions for active areas of research in NMR spectroscopy and imaging. The pseudospectral discretization framework is universal to solving optimal ensemble control problems arising in all areas of science and engineering, as demonstrated in recent extensions to neuroscience.[34]

Quantum systems are beset with parameters that show variation due to many environmental interactions. As more of these parameters are modeled to include this variation so as to properly characterize the physical system, it will be necessary to find ways to further optimize the discretization and sampling and reduce the computational complexity. In addition, while the pseudospectral method empirically exhibits convergence, a formal proof of convergence can be found for only a small class of systems.[32] We aim to extend the existing convergence results to a broader family of systems, which includes those studied for pulse design in quantum systems.

ACKNOWLEDGMENTS

This work was supported by the NSF under the Career Award #0747877 and the AFOSR Young Investigator Award FA9550-10-1-0146.

[1] J.-S. Li and N. Khaneja, Phys. Rev. A **73**, 030302 (2006).
[2] M. H. Levitt, Prog. Nucl. Magn. Reson. Spectrosc. **18**, 61 (1986).
[3] R. Tycko, N. Cho, E. Schneider, and A. Pines, J. Magn. Reson. **61**, 90 (1985).
[4] A. J. Shaka and R. Freeman, J. Magn. Reson. **55**, 487 (1983).
[5] M. Garwood and Y. Ke, J. Magn. Reson. **94**, 511 (1991).
[6] M. S. Silver and R. I. Joseph, Phys. Rev. A **31**, 2753 (1985).
[7] C. Yip, J. Fessler, and D. Noll, Magn. Reson. Med. **54**, 908 (2005).
[8] B. Pryor and N. Khaneja, J. Chem. Phys. **125**, 194111 (2006).
[9] J. Pauly, P. Le Roux, D. Nishimura, and A. Macovski, IEEE Trans. Med. Imaging **10**, 53 (1991).
[10] B. Pryor, "Fourier synthesis methods for identification and control of ensembles," Ph.D. thesis (Harvard University, 2007).
[11] S. Conolly, D. Nishimura, and A. Macovski, IEEE Trans. Med. Imaging **MI-5**, 106 (1986).
[12] N. Khaneja, T. Reiss, C. Kehlet, T. S. -Herbruggen, and S. J. Glaser, J. Magn. Reson. **172**, 296 (2005).
[13] Y. Ohtsuki, G. Turinici, and H. Rabitz, J. Chem. Phys. **120**, 5509 (2004).
[14] T. E. Skinner, T. Reiss, B. Luy, N. Khaneja, and S. J. Glaser, J. Magn. Reson. **163**, 8 (2003).
[15] N. Khaneja, J.-S. Li, C. Kehlet, B. Luy, and S. J. Glaser, Proc. Natl. Acad. Sci. U.S.A. **101**, 14742 (2004).
[16] D. P. Frueh, T. Ito, J.-S. Li, G. Wagner, S. J. Glaser, and N. Khaneja, J. Biomol. NMR **32**, 23 (2005).
[17] D. Stefanatos, S. J. Glaser, and N. Khaneja, Phys. Rev. A **72**, 062320 (2005).
[18] K. Kobzar, B. Luy, N. Khaneja, and S. Glaser, J. Magn. Reson. **173**, 229 (2005).
[19] J.-S. Li, J. Ruths, and D. Stefanatos, J. Chem. Phys. **131**, 164110 (2009).
[20] G. Elnagar, M. A. Kazemi, and M. Razzaghi, IEEE Trans. Autom. Control **40**, 1793 (1995).
[21] D. Manolopoulos, Chem. Phys. Lett. **152**, 23 (1988).
[22] I. Ross and F. Fahroo, in *New Trends in Nonlinear Dynamics and Control*, edited by W. Kang, M. Xiao, and C. R. Borges (Springer, Berlin, 2003), p. 327.
[23] F. Fahroo and I. Ross, J. Guid. Control Dyn. **24**, 270 (2001).
[24] C. Canuto, M. Y. Hussaini, A. Quarteroni, and T. A. Zang, *Spectral Methods* (Springer, Berlin, 2006).
[25] J. Boyd, *Chebyshev and Fourier Spectral Methods*, 2nd ed. (Dover, New York, 2000).
[26] G. Szego, *Orthogonal Polynomials* (American Mathematical Society, New York, 1959).
[27] P. Williams, ANZIAM J. **47**, C101 (2006).
[28] D. Gottlieb, Y. Hussaini, and S. Orszag, in *Spectral Methods for Partial Differential Equations*, edited by R. Voigt, D. Gottlieb, and M.Y. Hussaini (SIAM, Philadelphia, 1984), p. 1.
[29] J. Cavanagh, W. J. Fairbrother, A. G. Palmer III, M. Rance, and N. J. Skelton, *Protein NMR Spectroscopy* (Elsevier–Academic, Burlington, MA, 2007).
[30] N. Khaneja, T. Reiss, B. Luy, and S. J. Glasser, J. Magn. Reson. **162**, 311 (2003).
[31] N. Khaneja, B. Luy, and S. J. Glaser, Proc. Natl. Acad. Sci. U.S.A. **100**, 13162 (2003).
[32] Q. Gong, W. Kang, and M. Ross, IEEE Trans. Autom. Control **51**, 1115 (2006).
[33] See supplementary material at http://dx.doi.org/10.1063/1.3541253 for an example of AMPL code to solve the optimization problem in (16).
[34] J.-S. Li, in *Proceedings of the Eighth IFAC Symposium on Nonlinear Control Systems, Italy, September 2010* (International Federation of Automatic Control, Laxenburg, Austria, 2010).